

A method for correcting standard-based real-time PCR DNA quantitation when the standard's polymerase reaction efficiency is significantly different from that of the unknown's

Peter L. Irwin · Ly-Huong T. Nguyen · Chin-Yi Chen ·
Gaylen A. Uhlich · George C. Paoli

Received: 27 September 2011 / Revised: 7 January 2012 / Accepted: 11 January 2012 / Published online: 12 February 2012
© Springer-Verlag (outside the USA) 2012

Abstract Standard-based real-time or quantitative polymerase chain reaction quantitation of an unknown sample's DNA concentration (i.e., $[DNA]_{unk}$) assumes that the concentration dependence of the standard and unknown reactions (related to reaction efficiency, E) are equivalent. In our work with background food-borne organisms which can interfere with pathogen detection, we have found that it is generally possible to achieve an acceptable E (1 ± 0.05) for standard solutions by optimizing the PCR conditions, template purity, primer sequence, and amplicon lengths. However, this is frequently not true for the solutions containing unknown amounts of target DNA inasmuch as cell extracts are more chemically complex than the standards which have been amplified (2^{30} -fold) as well as undergone a purification process. When significant differences in E occur, it is not possible to accurately estimate unknown target DNA concentration from the standard solution's slope and intercept (from threshold cycle number, or C_T , versus $\text{Log}[DNA]$ data). What is needed is a standard-mediated intercept which can be specifically coupled with an unknown solution's PCR concentration dependence. In this work, we develop a simple mathematical procedure to generate a new standard curve with a slope ($\partial C_T / \partial \text{Log}[Dilution]_{unk}$) derived from at least three dilutions of the unknown target DNA solution ($[DNA]_{unk}$) and

an intercept calculated from the unknown's C_T s, DNA concentrations interpolated from the standard curve (i.e., the traditional estimate of $[DNA]_{unk}$), and $\partial C_T / \partial \text{Log}[Dilution]_{unk}$. We were able to achieve this due to our discovery of the predictable way in which the observed and ideal C_T versus $\text{Log}[DNA]$ slopes and intercepts deviate from one another. This "correction" in the standard-based $[DNA]_{unk}$ determination is typically 20–60% when the difference in the standard and unknown E is >0.1 .

Keywords Real-time PCR or qPCR · 16S rDNA or rRNA gene · DNA quantitation

Introduction

PCR is a temperature-modulated *Thermus aquaticus* DNA polymerase-catalyzed (*Taq*) [1] reaction used to amplify a few copies of DNA to many [2]. The PCR concept was "invented" in the early 1980s by Kary Mullis who was awarded the 1993 Nobel Prize in Chemistry for his efforts. Mullis' concept consisted of an admixture of several components which were already standard practices [2] such as the use of short lengths of single-stranded DNA (ssDNA) as primers for the DNA polymerase (extracted and purified from *Escherichia coli* at this stage of development). The innovation of Mullis' concept was in the juxtaposition of two (forward and reverse) primers which are complementary to the two opposing strands of ssDNA and which specifically amplify the double-stranded target DNA (dsDNA) between these primers. Thus, during each temperature modulation cycle (C), the concentration of this targeted DNA region is doubled and products from each C can act as targets during the next C . Of course, there have been many significant technological improvements (e.g., heat-stable, *Taq* polymerases

Reference to a brand or firm name does not constitute endorsement by the U.S. Department of Agriculture over others of a similar nature not mentioned. The USDA is an equal opportunity provider and employer.

P. L. Irwin (✉) · L.-H. T. Nguyen · C.-Y. Chen · G. A. Uhlich ·
G. C. Paoli

Molecular Characterization of Foodborne Pathogens,
Eastern Regional Research Center, Agricultural Research Service,
United States Department of Agriculture,
600 E. Mermaid Lane,
Wyndmoor, PA 19038, USA
e-mail: peter.irwin@ars.usda.gov

which allow for a closed thermocycler system) made by others [2, 3] before a modern PCR system was attained.

In brief, the basic PCR experiment is made up of programmed temperature variations known as “thermal cycling” (or “thermocycling”) and consists of repeated cycles of heating and cooling of the reaction mixture containing *Taq* polymerase [1] (a thermostable DNA polymerase), buffer, forward and reverse primers (each ~15–20 nucleotides in length and complementary to a defined sequence on each of the two strands of denatured DNA), nucleotide triphosphates (NTPs), a dsDNA target, etc. Each thermal cycle (*C*) starts with denaturation (typically ~30 s at ~95 °C) of the dsDNA into its complementary ssDNA components. This is followed by annealing (customarily ~45 s at ~55 °C), whereupon the forward and reverse primers bind to each complementary target’s ssDNA. The third and final part of each *C* is the extension phase (routinely ~60 s at ~72 °C), at which point NTPs are covalently bonded as deoxyribose phosphate esters to the 3’ terminus of each annealed primer in a sequential fashion effectively doubling the targeted dsDNA population after each cycle [4]. For example, if the typical end-point PCR experiment uses 30 Cs, then $[DNA]_{30} = [DNA]_0 \times 2^{30} \sim 10^9$ DNA [5] copies (assumes a 100% efficient reaction) for every target DNA molecule present in the starting solution.

DNA-based detection methods, such as PCR, are the most sensitive [6] biosensor approaches available as they have the ability, in theory at least, to detect one gene copy per volume tested. With appropriately designed primers, PCR can be highly specific [4] in the detection and identification of specific organisms such as various *Campylobacter* species in problematic food [7] samples. Most end-point PCR users rely on the detection of the reaction’s product (“amplicon”) with gel electrophoresis and a set of molecular size-based DNA standards (i.e., a DNA “ladder”); this form of PCR is qualitative. Thus, a PCR product of appropriate size should be apparent *only* if the target DNA strand is present to begin with. The quantitative version is known as *real-time* or *quantitative* PCR (qPCR; the acronym “RT” is generally reserved for “reverse transcriptase”) and is one of the few techniques which have the potential to quantify exceedingly low concentrations [i.e., ~1 copy per volume used (typically 1 μL) or approx. 3×10^{-18} M] of genomic DNA based upon comparisons of results for an unknown (unk) relative to several standard (stnd) serially diluted targets. There are two major classes of qPCR [5, 8]: standard-based and relative. In standard-based quantitation, the gene copy number of the unk is calculated based upon comparisons with a set of stnd solutions which are, in this work, purified amplicons of the target gene. With relative quantitation, the unk’s concentration is estimated relative to another gene (of known copy number per genome) in the test genome based upon the ratio of their PCR responses.

Both forms of qPCR assume that the stnd targets, or comparison genes, being amplified have similar polymerase reaction efficiencies and that all copies in the sample are available for amplification. However, real-time PCR can also be of value as a simple detection method (disregarding the quantitative aspects) especially for multiplex PCR experiments (i.e., more than one target gene) [7]. Since such a multiplex procedure does not rely on molecular size standards, primers can be designed without concern for differentiating product size because specific amplicon detection relies on the fluorescence specificity of the detection probe. This form of binomial (+ or –) detection system has recently [9] been proposed for a multiplex qPCR most probable number quantification of various food-borne pathogens (e.g., *Campylobacter* species) which occur in such small numbers that a large number of technical replicates would be required to accurately determine their concentration using qPCR quantitation alone.

All standard-based qPCR determinations of unknown, or target, DNA concentration ($[DNA]_{unk}$) assume that the concentration dependence of the stnd ($\partial C_T / \partial \text{Log}_\beta [DNA]_i = \partial C_T / \partial \text{Log}_\beta \phi^i = \text{Slope}_{\beta i}$) and unk ($\partial C_T / \partial \text{Log}_\beta \phi^j = \text{Slope}_{\beta j}$) reactions are equivalent (see “**Terminology and definitions**”). We have found that this assumption is frequently not true. In fact, an unk extract’s observed rate of C_T changes with respect to the base β logarithm of several dilutions ($\text{Slope}_{\beta j}$) is rarely reported. While it is generally possible to achieve an acceptable *Taq* polymerase efficiency ($E_{stnd} = -1 + \beta^{-1/\text{Slope}_{\beta i}} = 1.0 \pm 0.05$) for standards by optimizing the PCR conditions, primer characteristics, template purity, and amplicon lengths [6, 10], this is not necessarily true for solutions containing unknown target DNA ($E_{unk} = -1 + \beta^{-1/\text{Slope}_{\beta j}}$). In fact, various theoretical (e.g., *E* affected by the ratio of free to total *Taq* DNA polymerase) [11] and empirical considerations (e.g., *E* affected by baseline estimation errors) [12] need to be addressed in order to assume *E* equivalency [11, 13, 14] between stnd and unk solutions. Unfortunately, cell-free DNA extracts are far more complex than qPCR standards which typically are an amplified (10^9 -fold; i.e., 30 cycles) product which has undergone a purification step, and therefore, unk DNA solutions may show polymerase reaction efficiencies which are substantially different than E_{stnd} . When significant differences in polymerase reaction efficiency occur between stnd and unk, it is impossible to accurately estimate $[DNA]_{unk}$ from stnd solutions ($[DNA]_i$) since such estimations rely both on a *slope* ($= \partial C_T / \partial \text{Log}_\beta [DNA]_i = \text{Slope}_{\beta i} = \Sigma xy \div \Sigma x^2$; $x = X - \bar{x}$ and $y = Y - \bar{y}$; $X = \text{Log}_\beta [DNA]_i$; $Y = C_T$; \bar{x} = average *X*; \bar{y} = average *Y* = \bar{C}_T) and an *intercept* ($C_{T \text{ int obs}} = \bar{y} - \{ \Sigma xy \div \Sigma x^2 \} \bar{x}$) [15] which are mathematically interrelated. What is needed is a stnd-based intercept ($C_{T \text{ int predicted}}$) which can be specifically associated with an unk’s relative

concentration dependence or Slope_{β^j} : i.e., a new std curve with the slope based upon at least three dilutions of the unk and an intercept calculated from the unk C_T s and their associated [DNA]s which have been interpolated from the standard curve, and Slope_{β^j} . In this work, we describe such a calculation that is experimentally applied to two crude DNA extracts which show significant deviations (i.e., $E_{\text{std}} \neq E_{\text{unk}}$) from the std results and two others with C_T - Log_{β^j} dependencies closer to the standards (i.e., $E_{\text{std}} \sim E_{\text{unk}}$).

Materials and methods

16S rDNA (i.e., the rRNA “gene”) amplification

Two strains of Gram-positive (*Brochothrix thermosphacta* and *Carnobacteria maltaromaticum*) and two strains of Gram-negative (*Shigella sonnei* and *Serratia proteamaculans*) bacteria were streaked onto Luria–Bertani (LB) agar plates and grown for 24–36 h at room temperature (~20–22 °C) before a single colony was selected. All strains were previously isolated from commercially available ground chicken and identified based upon rRNA “gene” (16S rDNA) sequencing [16]. Each selected colony was mixed with 50 μL PrepMan Ultra (Applied Biosystems, Foster City, CA, USA), heated at ~100 °C for 15 min, centrifuged, and the supernatant collected into a fresh microfuge tube. Each PCR mixture contained 25 μL GoTaq Green 2X (Promega, Madison, WI, USA), 5 μL (10 μM) each of EubA and EubB [17], 14 μL PCR water (i.e., free of all DNA, RNase, and DNase contamination; Qiagen Sciences, Germantown, MD, USA), and 1 μL template DNA. Thermocycler (iCycler, BioRad, Hercules, CA, USA) conditions were as follows:

- Cycle 1 (1 \times): 90 s at 95 °C
- Cycle 2 (30 \times): Step 1: 30 s at 95 °C
Step 2: 45 s at 55 °C
Step 3: 60 s at 72 °C
- Cycle 3 (1 \times): 5 min at 72 °C
- Cycle 4 (1 \times): 4 °C until needed

Upon determining the presence of 16S rDNA via gel electrophoresis (an approx. 1,500-bp product), the PCR products were cleaned using AmPure magnetic beads (Agencourt Bioscience, Beverly, MA, USA). This protocol called for 81 μL of the magnetic beads to be mixed with the PCR sample followed by magnetic separation of the bead–DNA complex (SPRIplate 96-R magnetic plate) for 20 min. The supernatant liquid was carefully removed, discarded, and the beads washed while still on the magnetic plate with 150 μL of 70% EtOH for 30 s, after which the EtOH was carefully removed. A second wash was performed as above and the magnetic beads were allowed to air-dry at room temperature for about 45 min. Once dry, 40 μL PCR water

was introduced and allowed to settle. The beads were again separated on the magnet and 20 μL of the supernatant (a “cleaned” amplicon solution) was collected and stored in a fresh tube at –20 °C. Such purified PCR amplicons were used throughout this work. Concentration of these DNA stds ([DNA]_{*i*}) was determined using a NanoDrop ND-1000 UV–VIS Spectrophotometer (NanoDrop Technologies Inc., Wilmington, DE, USA) where 2 μL of undiluted, purified PCR product was placed onto the apparatus and the OD measured ($\lambda=260$ nm). OD₂₆₀ values were converted to concentration (nanograms DNA per microliter) by comparing them with solutions of known DNA concentration (approx. 67, 50, 38, 28, 21, 16, 12, and 0.0 ng μL^{-1} of Lambda DNA *Hind*III digest; Sigma-Aldrich, St. Louis, USA). Dilutions were made on this original cleaned-up std so that the final concentration of DNA was between 10⁸ and 10⁹ copies per microliter, which was used as the undiluted qPCR std solution.

qPCR experimental procedures

Sheared salmon sperm DNA (Ambion, Austin, TX, USA) was used to suppress the apparent binding of std or unk DNA to the walls of the mixing tubes (RNase/DNase/pyrogen-safe Denville Scientific, Posi-Click, 1.7-mL polypropylene microfuge tubes). The salmon sperm DNA (10 mg/mL) was diluted so that the final concentration was 4 ng per reaction.

The QuantiFast SYBR Green kit (Qiagen Sciences) was utilized where each reaction contained 10 μL 2 \times QuantiFast SYBR green, 2.5 μL of a 10- μM stock solution of each forward and reverse primers (all primers [5'→3'] were selected to produce no other than the desired amplicon; *Brochothrix*: forward=CACAGCTGGGGATAACATCGA, reverse=GGTCAGACTTTCGTCCATTGCC, 262-bp product; *Shigella*: forward=TTAGCTCCGGAAGCCACG, reverse=ATACTGGCAAGCTTGAGTCTCGT, 226-bp product; *Serratia*: forward=CTGAACCCTTCCTCCTCGCTG, reverse=GCTCTCTGGGTGACGAGC, 375-bp product; *Carnobacterium*: forward=CGTGCCTAATACATGCAAG, reverse=AGCCACCTTTCCTTCAAG, 180-bp product), 4 μL PCR H₂O, and 1 μL template DNA. All experiments were run on an Applied Biosystems FAST 7500 (Carlsbad, CA, USA), and the conditions were programmed according to the QuantiFast SYBR green protocol (Qiagen Sciences):

- Cycle 1 (1 \times): 95 °C for 5 min
- Cycle 2 (40 \times): Step 1: 95 °C for 10 s
Step 2: 60 °C for 30 s

The third cycle (not shown) is related to the acquisition of the DNA melt curve [18]. The melt curve data were utilized in every experiment to verify that the appropriate PCR product was being amplified.

rRNA gene (16S rDNA) cloning

The four bacterial strains (*Brochothrix*, *Carnobacteria*, *Shigella*, and *Serratia*) were streaked onto LB plates and grown 24–36 h at room temperature before a single colony was picked. Genomic DNA was extracted by mixing an isolated colony with 50 μL PrepMan Ultra (Applied Biosystems), heated at $\sim 100^\circ\text{C}$ for 15 min, centrifuged, and the supernatant collected into a fresh microfuge tube. The Qiagen Multiplex PCR kit (Qiagen Sciences) was utilized to make PCR products for cloning. According to the Qiagen protocol, each reaction contained: 25 μL 2 \times Qiagen Multiplex PCR Master Mix, 5 μL each of 2 μM EubA and EubB [17], 5 μL 5 \times “Q-Solution,” 9 μL PCR water and 1 μL template DNA. The thermocycling conditions were:

- Cycle 1 (1 \times): 15 min at 95°C initial activation step
- Cycle 2 (30 \times): Step 1: 30 s at 94°C
Step 2: 90 s at 57°C
Step 3: 90 s at 72°C
- Cycle 3 (1 \times): 10 min at 72°C
- Cycle 4 (1 \times): 4°C until needed

After amplification of the rRNA gene targets, gel electrophoresis was performed to confirm that the calculated and observed product sizes matched whereupon 16S rDNA cloning proceeded. TOPO TA Cloning kit pCR 2.1-TOPO vector (Invitrogen, Carlsbad, CA, USA) was used and each of the four reaction mixes contained: 2 μL 16S rDNA PCR product, 1 μL Invitrogen proprietary “salt solution,” 1 μL TOPO vector (pCR2.1), and 2 μL PCR water for a total of 6 μL . These solutions were incubated at 25°C for 30 min and placed on ice. Once chilled, 2 μL of the TOPO reaction mixture was added to 50 μL of “One Shot Max Efficiency” *E. coli* DH5 α -T1 chemically competent cells and incubated on ice for an additional 30 min. The reaction was then heat-shocked in a H_2O bath set at 42°C for 90 s and placed back on ice for another 5 min, after which 1 mL of LB was added. This mixture was incubated at 37°C with shaking at 200 rpm for 45 min, whereupon 100 μL of reaction mix was plated onto dried LB/Kan/Xgal 1.5% agar plates (50 $\mu\text{g}/\text{mL}$ kanamycin and 40 $\mu\text{g}/\text{mL}$ Xgal). The plates were then incubated overnight at 37°C .

From each of the above clones plated onto LB/Kan/Xgal agar, at least four colonies were picked and inoculated into 4 mL of LB broth and cultured overnight at 37°C with shaking. To purify the plasmid DNA, QIAprep miniprep (Qiagen Sciences) was used according to the manufacturer’s protocol: 1.5 mL of overnight culture was spun down and the pellet resuspended in 250 μL buffer “P1”; 250 μL buffer “P2” was then added and gently mixed by inverting the tubes four to six times; 350 μL buffer “N3” followed and was immediately mixed; the tubes were centrifuged (5415R

refrigerated centrifuge, Eppendorf AG, Hamburg, DE) at 13,000 rpm for 10 min; the supernatant was placed into a QIAprep spin column, centrifuged for 90 s, and the flow-through was discarded; the extracted DNA was washed with 750 μL buffer “PE,” centrifuged again for 90 s, and the flow-through was discarded; the samples were re-centrifuged for an additional minute; the QIAprep column was positioned into a fresh microfuge tube and 50 μL 1 \times TE (Tris/EDTA) buffer was pipetted into the middle of the column/filter; after 1 min, the tube was centrifuged and the plasmid DNA prep was collected.

Sequencing of cloned rRNA genes

Before sequencing the cloned 16S rDNA targets, the absorbance was measured using a NanoDrop ND-1000 UV–VIS Spectrophotometer and the approximate DNA concentration determined as described above (“16S rDNA amplification”). All samples contained $\sim 200\text{ ng } \mu\text{L}^{-1}$ plasmid DNA and were used as the template for four sets of sequence reactions using primers M13F and M13R (residing in the vector just outside the cloned region, provided with the cloning kit) and 519F and 519R (within the cloned 16S rDNA moiety). For M13F and M13R primers, each reaction contained: 10.5 μL PCR water, 7 μL 2.5 \times sequence reaction buffer (Applied Biosystems), 0.5 μL of 100 $\text{ng } \mu\text{L}^{-1}$ primer, 1 μL Big Dye terminator cycle sequencing reagent mixture (v3.1 Applied Biosystems), and 1 μL template DNA. For the 519F and 519R [17] internal 16S rDNA primers, each reaction contained 10 μL PCR water, 7 μL 2.5 \times sequence reaction buffer (Applied Biosystems), 1 μL of 3.2 μM primer, 1 μL Big Dye terminator cycle sequencing reagent mixture (Applied Biosystems), and 1 μL template DNA. Sequence reaction conditions were as follows:

- Cycle 1 (1 \times): 5 min at 95°C
- Cycle 2 (30 \times): Step 1: 10 s at 96°C
Step 2: 5 s at 55°C
Step 3: 4 min at 60°C
- Cycle 3 (1 \times): 4°C until needed

Sequence reactions were cleaned using CleanSeq magnetic beads (Agencourt Bioscience) where 8 μL of CleanSeq was added, thoroughly mixed, and 60 μL of 85% ethanol was subsequently added. The samples were then magnetically separated for 5 min and the supernatant discarded. Another wash with 100 μL of 85% ethanol was introduced to the beads and the supernatant was again discarded after 30 s. The samples were air-dried at room temperature for about 30–45 min, after which 40 μL of PCR water was added to separate the DNA from the beads. Beads were magnetically separated for another 5 min, and 20 μL was collected for sequencing.

Sequence data were gathered using an Applied Biosystems 3930 DNA analyzer and edited using Sequencher software (Gene Codes, Ann Arbor, MI, USA).

Restriction enzyme digestion of the cloned amplicons

NEBCutter (v2.0) was used to find a restriction endonuclease site outside the cloned 16S rDNA moiety. *Bam*HI endonuclease (New England Biolabs, Ipswich, MA, USA) was chosen to linearize all plasmids. Each 20 μ L reaction contained 2 μ L 10 \times NEB #2 buffer, 2 μ L 10 \times BSA, 10 μ L H₂O, 1 μ L *Bam*HI enzyme, and 5 μ L plasmid DNA. The samples were incubated for 3 h at 37 °C. The linearized plasmids were ~6 kbp and were cleaned using Qiagen MiniElute PCR purification kit (Qiagen Sciences). The protocol was as follows: 5 volumes of buffer “PB” to 1 volume of the above digestion solution were mixed and placed into refrigerated columns provided. The sample was centrifuged at the maximum speed for 1 min and flow-through discarded. Seven hundred fifty microliters of buffer “PE” was added to the column and the flow-through again discarded after centrifugation. The column was placed into a clean microfuge tube where 10 μ L buffer “EB” was placed onto the center of the membrane to let stand for 1 min, and then centrifuged for 1 min to collect the purified DNA. The purified linear (or “cut”) DNA, which was quantified as discussed previously (in “rRNA gene amplification”), serves as the template for qPCR reactions.

Results and discussion

Terminology and definitions

Indices

The superscript/subscript “*i*” represents the different serial dilutions of standard DNA solutions, whereas “*j*” represents the different dilutions of unknown extract solutions. For example, serial dilution factors are represented as either ϕ^i (std) or ϕ^j (unk), whereupon ϕ is characteristically 0.1 (i.e., 1:10 dilutions). Thus, for $i=0$ and $\phi=0.1$, the dilution factor ϕ^0 is 1 (no dilution); for $i=4$, $\phi^4=0.1^4=10^{-4}$, etc. In some results presented herein, there are numerous (10 experimental replicates/amplicon \times 4 amplicons) individual experiments that contain several *i* dilutions, where each individual dilution set (an experimental unit) is assigned a number associated with the index *k*. Thus, as an illustration, *Brochothrix*-based 16S rDNA stnds (circles throughout) could be assigned the experimental index $k=1-10$, *Shigella*-based stnds (diamonds) $k=11-20$, *Serratia*-based stnds (squares) $k=21-30$, and *Carnobacterium*-based stnds (triangles) $k=31-40$.

Observed δC_T

Figure 1 displays the qPCR results from seven 1:10 serial dilutions of a std solution of *Brochothrix* (isolated from ground chicken) [16] rDNA amplicons (approx. 1,500 bp) using primers which give a 262-bp product (“Methods”). The results in Fig. 1a show the relative, normalized fluorescence signal (R_N) detected by the qPCR thermocycler as a function of *C*. Since only one set (forward and reverse) of primers (i.e., one gene) was utilized, a nonspecific DNA dye was used (e.g., SYBR Green I=*N,N'*-dimethyl-*N*-[4-[(*E*)-(3-methyl-1,3-benzothiazol-2-ylidene)methyl]-1-phenylquinolin-1-ium-2-yl]-*N*-propylpropane-1,3-diamine) which binds to the minor groove [19] of dsDNA and fluoresces ($\lambda_{max}=488$ nm absorption maximum, $\lambda_{max}=522$ nm emission maximum). In Fig. 1a, b, the dotted horizontal line is the R_N threshold. This threshold line is determined by the Applied Biosystem’s FAST 7500 qPCR instrumental software and shows when the reaction reaches sufficient fluorescent intensity change ($\Delta R_N=R_N-R_{baseline}$, a semi-log plot of which is displayed in Fig. 1b) above the background during the exponential phase of the DNA amplification. The cycle at which the sample reaches this level is called the threshold cycle number (C_T). The dotted vertical lines in Fig. 1a, b are the interpolated C_T s at each dilution and are semi-log plotted in Fig. 1c against various levels of target DNA copy number per assay ($[DNA]_i$). The absolute value of the difference between the adjacent C_T s defines δC_{T_i} (i.e., $C_{T_i}-C_{T_{i-1}}=\delta C_{T_i}$), whereupon C_{T_i} is the *i*th dilution’s C_T and $C_{T_{i-1}}$ is the C_T associated with the $[DNA]$ which was used to make the *i*th dilution. Ideally, each δC_{T_i} should be equivalent to any other. The experimental average of all δC_T s should also be approximately equivalent to the absolute value of the slope ($|\partial C_T/\partial \text{Log}_\beta [DNA]_i|$ or $|\partial C_T/\partial \text{Log}_\beta \phi^i|=|\text{Slope}_\beta i|$) of the C_T versus $\text{Log}_\beta [DNA]_i$ or $\text{Log}_\beta \phi^i$ dependency (Fig. 1c), but only when the logarithm’s base β is equal to ϕ^{-1} .

Ideal δC_T

The symbol $[DNA]_i$ represents the *i*th dilution of a std DNA solution in units of copies per qPCR assay (usually 1 μ L in a total PCR volume of about 20 μ L); that is, $[DNA]_i=\phi^i \times [DNA]_0$, where $[DNA]_0$ is the undiluted (i.e., $i=0$), or starting, std solution. Ideally, the DNA concentration at any two adjacent C_T s is

$$\begin{aligned}
 [DNA]_{C_{T_{i-1}}} &= [DNA]_{i-1} 2^{C_{T_{i-1}}} \\
 \text{and} & \\
 [DNA]_{C_{T_i}} &= [DNA]_i 2^{C_{T_i}}
 \end{aligned}
 \tag{1}$$

because the starting concentrations ($[DNA]_i$ or $[DNA]_{i-1}$) double during each thermocycle *C*. Upon rearranging Eq. 1, an ideal δC_T can be formulated

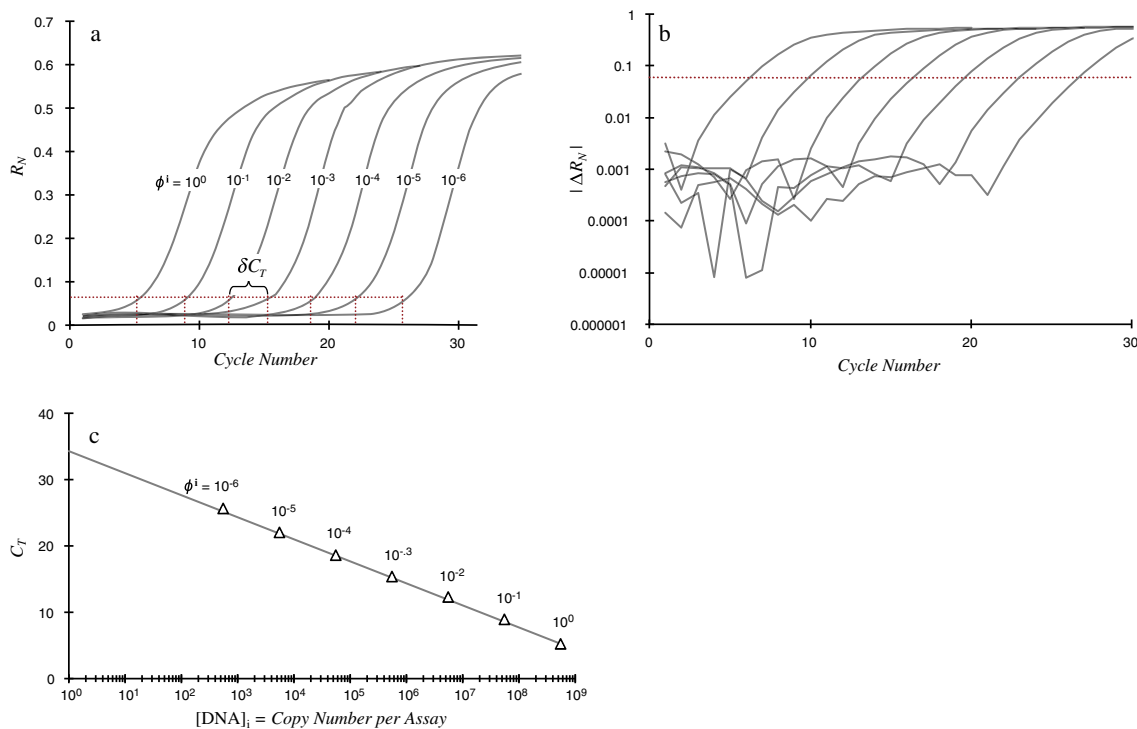


Fig. 1 **a** Graph of R_N with cycle number (C) for seven dilutions of *Brochothrix* 16S rDNA PCR products. **b** Graph of the absolute value of the fluorescent intensity change as a function of C showing the

placement of the threshold. **c** Graph of threshold cycle number (C_T) as a function of $[DNA]_i$ for various dilutions of *Brochothrix* 16S rDNA PCR products ($E=0.997$, $\delta C_T=|\text{Slope}_\beta|=3.33$)

$$\delta C_T = C_{Ti} - C_{T(i-1)} = \text{Log}_2 \frac{[DNA]_{C_{Ti}} [DNA]_{i-1}}{[DNA]_i [DNA]_{C_{T(i-1)}}}$$

Simplification of the above results in

$$\delta C_T = \text{Log}_2 \frac{[DNA]_{i-1}}{[DNA]_i} = \text{Log}_2 \phi^{-1} = -\text{Log}_2 \phi \tag{2}$$

because the $[DNA]$ at any C_T is approximately equivalent [5] (i.e., $[DNA]_{C_{Ti}} \approx [DNA]_{C_{T(i-1)}}$).

Ideal $C_{T\text{ obs}}$ versus $\text{Log}_\beta [DNA]_i$ slope

In the linear estimation of the regression parameters displayed in Fig. 1c, $\text{Slope}_\beta i$ is ideally related to δC_T as follows

$$\begin{aligned} \frac{\partial C_T}{\partial \text{Log}_\beta [DNA]_i} &\sim \frac{\delta C_T}{\delta \{ \text{Log}_\beta [DNA]_i \}} = \frac{-\text{Log}_2 \phi}{\text{Log}_\beta \frac{[DNA]_i}{[DNA]_{i-1}}} \\ &= \frac{-\text{Log}_2 \phi}{\text{Log}_\beta \phi} = -\frac{\text{Ln } \phi}{\text{Ln } 2} \frac{\text{Ln } \beta}{\text{Ln } \phi} = -\frac{\text{Ln } \beta}{\text{Ln } 2} = -\text{Log}_2 \beta \end{aligned} \tag{3}$$

If the above logarithm's base (β)= ϕ^{-1} , then $\delta C_T \sim |\text{Slope}_\beta| \sim \text{Log}_2 \beta = -\text{Log}_2 \phi$; under all circumstances,

$$\frac{\partial C_T}{\partial \text{Log}_\beta [DNA]_i} = \frac{\partial C_T}{\partial \text{Log}_\beta \phi^i} = \text{Slope}_\beta i. \tag{4}$$

The departure from ideal behavior is usually represented by the degree to which the PCR efficiency (E) deviates from unity

$$\begin{aligned} E_{std} &= -1 + \beta^{-1/\text{Slope}_\beta i} \\ \text{or} & \\ E_{unk} &= -1 + \beta^{-1/\text{Slope}_\beta j} \end{aligned} \tag{5}$$

thus, $\text{Slope}_\beta i = -\text{Log}_{(1+E_{std})} \beta$ and $\text{Slope}_\beta j = -\text{Log}_{(1+E_{unk})} \beta$ (i.e., equivalent to Eq. 3 when $E=1$).

Ideal C_T versus $\text{Log}_\beta [DNA]_i$ intercept

The ideal intercept (i.e., $C_{T\text{ int ideal}}$ =idealized C_T at $[DNA]=1$ copy per assay or the C_T at $\text{Log}_\beta [DNA]=0$) of the C_T versus $\text{Log}_\beta [DNA]_i$ dependency is derived by taking the ideal slope between C_T at $\text{Log}_\beta [DNA]_i$ and C_T at $\text{Log}_\beta [DNA]=0$; thus, ideally,

$$-\text{Log}_2 \beta = \frac{C_{T\text{ int ideal}} - C_{Ti}}{\text{Log}_\beta \frac{1}{[DNA]_i}} = -\frac{C_{T\text{ int ideal}} - C_{Ti}}{\text{Log}_\beta [DNA]_i}$$

and

$$\text{Log}_2 \beta = \frac{C_{T\text{ int ideal}} - C_{Ti}}{\text{Log}_\beta [DNA]_i}$$

A rearrangement gives

$$C_{T \text{ int ideal}} = \frac{\text{Ln } \beta}{\text{Ln } 2} \frac{\text{Ln} [\text{DNA}]_i}{\text{Ln } \beta} + C_{T_i} \tag{6}$$

$$= \frac{\text{Ln} [\text{DNA}]_i}{\text{Ln } 2} + C_{T_i} = C_{T_i} + \text{Log}_2 [\text{DNA}]_i.$$

Figure 1c is replotted in Fig. 2 with the above (Eqs. 3 and 6 for the slope and intercept, respectively) ideal regression lines associated with each std's C_{T_i} at $\text{Log}_{10}[\text{DNA}]_i$. Because these data have a nearly perfect E , the variably colored lines (slopes= $-\text{Log}_2 10$; each i th point's intercept= $C_{T_i} + \text{Log}_2 [\text{DNA}]_i$) are nearly equivalent to that of the linear estimate. The inset plot in Fig. 2 gives an idea of this closeness from the standpoint of these $C_{T \text{ int ideal}}$ (Eq. 6) values.

The relationship between ideal and observed $C_{T \text{ int obs}}$ and $\text{Slope}_{\beta i}$

Much of the data discussed in this work were derived from the same ten qPCR experiments (one full set of dilutions for each amplicon repeated ten times) using purified EubA- and EubB-based [17] 16S rDNA amplicons from four different organisms (4 amplicons \times 7 dilutions/amplicon \times 10 replicates/dilution = 280 total C_T observations) from which the average C_T (\bar{C}_T , main graph) and E (\bar{E} , inset) were gleaned (Fig. 3). The standard deviations for each \bar{C}_T in Fig. 3 are not shown inasmuch as they are less than or equal to the size of the plotted symbol; however, the experimental coefficients of variation ($\text{CV} = \sqrt{\text{EMS}} \div \bar{C}_{T \text{ total}}$; EMS =error mean square; $\bar{C}_{T \text{ total}}$ = the experimental \bar{C}_T across 7 concentrations \times 10 replicates = $\sum_{ik} C_{T_{ik}} \div 70$) were 0.494% for the *Shigella* 16S rDNA amplification product ($\bar{C}_{T \text{ total}} = 16.2$), 0.541% for *Carnobacterium* ($\bar{C}_{T \text{ total}} = 16.9$), 0.612% for *Brochothrix* ($\bar{C}_{T \text{ total}} = 15.9$),

and 0.708% for *Serratia* ($\bar{C}_{T \text{ total}} = 16.7$). These results show the relatively low error associated with these types of experiments from the standpoint of the same std solutions. Slightly different results would be observed from another set of prepared standards (as shown later on in this work). The inset in Fig. 3 represents the results of the analysis of variance for these E_{stds} ; when the \bar{E} error bars ($\pm s_{\bar{E}} \times q_{0.05} \div 2$; $s_{\bar{E}} = \sqrt{\text{EMS} \div 10}$) overlap, the \bar{E} values are considered *not* to be significantly different at the $P=0.05$ level; therefore, $\{\bar{E}(\textit{Shigella}) \sim \bar{E}(\textit{Brochothrix})\} \neq \{\bar{E}(\textit{Carnobacterium}) \sim \bar{E}(\textit{Serratia})\}$.

Using expressions in Eqs. 3 and 6 (ideal C_T versus $\text{Log}_{\beta} [\text{DNA}]_i$ slope and intercept, respectively), Fig. 4 is a plot of $Y = \{C_{T \text{ int obs}} - C_{T \text{ int ideal}}\} = C_{T \text{ int obs}} - (C_{T_i} + \text{Log}_2 [\text{DNA}]_i)$ as a function of $X = \{|\text{Slope}_{\beta i}| - \text{Log}_2 \beta\}$ for the aforementioned ten experimental replicates of each qPCR experiment using rDNA amplicons from four different organisms. Figure 4 is thus a plot of deviations from ideality for the empirically derived C_T versus $\text{Log}_{\beta} [\text{DNA}]_i$ slopes and intercepts for $\beta=2$ (closed symbols) or 10 (open symbols). While Fig. 3 demonstrates how small the within-amplicon variation (between replicates) is, Fig. 4 proves that there is still enough variation to easily discern a relationship between the observed and ideal difference for $|\text{Slope}_{\beta i}|$ and $C_{T \text{ int}}$. The linear regression-based slopes associated with the plots in Fig. 4 (observed $\partial Y/\partial X \sim 25.7$ and 7.73 for $\beta=2$ and 10, respectively) were equivalent to the average base β logarithm of the three $[\text{DNA}]_i$ values ($\sum_{i=0}^2 (\text{Log}_{\beta} [\text{DNA}]_i) \div 3 = 25.7$ and 7.72 for $\beta=2$ and 10) which were used to calculate $C_{T \text{ int ideal}}$ (Eq. 6). The intercepts (i.e., those experiments where $E \sim 1$) in Fig. 4 were all ~ 0 .

From all k experimental sets ($k=1-40$: 10 qPCR experiments/species \times 4 species; each k th experiment contained seven i dilutions; Figs. 3 and 4) of std 16S $[\text{DNA}]_i$ s and their resultant linear regression parameters (each k th slope and intercept = $\{\partial C_{T_i} / \partial \text{Log}_{\beta} [\text{DNA}]_i\}_k = \text{Slope}_{\beta i_k}$ and

Fig. 2 Plot of threshold cycle number C_{T_i} as a function of $[\text{DNA}]_i$ for various dilutions of *Brochothrix* 16S rDNA PCR products as shown in Fig. 1c. The variously colored lines extending from each data point represent the ideal slope (Eq. 3) and intercept (Eq. 6) at each individual $[\text{DNA}]_i$ value. The inset figure is a blowup of the Y-axis showing the closeness of all the idealized C_{T_i} versus $[\text{DNA}]_i$ intercepts, relative to the observed intercept shown as an open circle, when E is close to unity

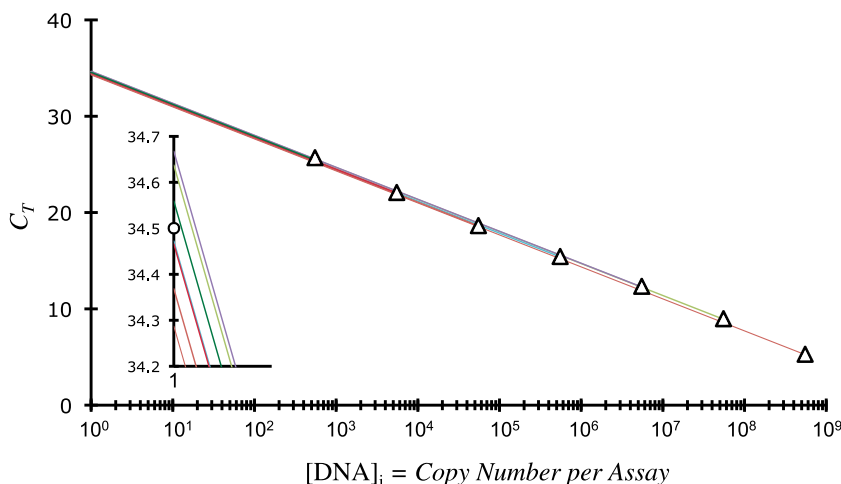
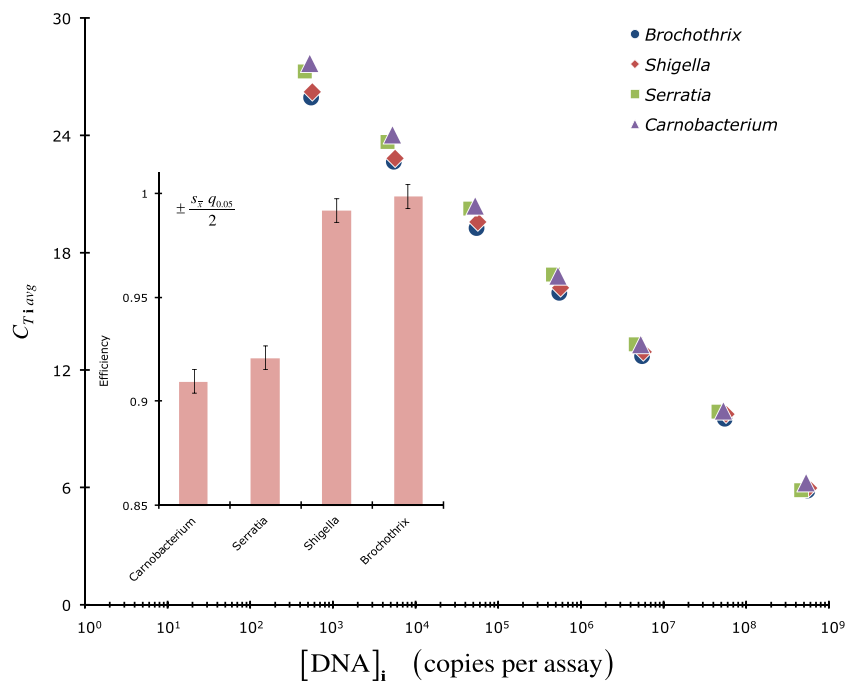


Fig. 3 Graph representing all the average C_{Ti} 's ($n=10$) used in this work for the four types of 16S rDNA PCR products. The inset bar graph is a plot of the average E for each of the species' ($Brochothrix=0.998$; $Shigella=0.992$; $Carnobacterium=0.910$; $Serratia=0.921$) cleaned-up PCR 16S rDNA amplicons; overlapping error bars are not significantly different at the $P=0.05$ level



$C_{T\text{int obs } k}$, respectively), 40 new sets of C_T values ($C_{T\text{fixd } k}$) at various fixed $[DNA]$ ($[DNA]_{\text{fixd}}=10^4, 10^5, 10^6, 10^7, \text{ or } 10^8$ copies per assay) were calculated. From these $C_{T\text{fixd } k}$ and associated $[DNA]_{\text{fixd}}$, new $C_{T\text{int ideal } k}$ ($C_{T\text{fixd } k} + \text{Log}_2[DNA]_{\text{fixd}}$; Eq. 6) were calculated. Figure 5 displays the resultant 40 $C_{T\text{int obs } k} - C_{T\text{int ideal } k}$ values plotted as a function of $\{|\text{Slope}_{\beta i}| - \text{Log}_2 \beta\}$, whereupon the $\text{Slope}_{\beta i}$ values were those associated with the original linear relationships, the average of which are shown in Fig. 4. The most significant

point to be made is that the $\partial Y/\partial X$ values in Fig. 5, in this recalculation of the linear estimates in Fig. 4, were exactly equal to the base β logarithm of each $[DNA]_{\text{fixd}}$ which was used to calculate the new $C_{T\text{int ideal } k}$. The slopes in Fig. 5 associated with the $\beta=2$ or 10 log transformations were 13.3 or 4.00 for $[DNA]_{\text{fixd}}=10^4$; 16.6 or 5.00 for $[DNA]_{\text{fixd}}=10^5$; 19.9 or 6.00 for $[DNA]_{\text{fixd}}=10^6$; 23.3 or 7.00 for $[DNA]_{\text{fixd}}=10^7$; and 26.6 or 8.00 for $[DNA]_{\text{fixd}}=10^8$ (three significant figures). Clearly, the $\partial Y/\partial X$ numerical results represented in

Fig. 4 Deviations from ideality for the C_{Ti} versus $\text{Log}_{\beta}[DNA]_i$ intercepts (Y -axis) and $|\text{slopes}|$ (X -axis). The data used for this figure were derived from the individual experimental components making up the averages present in Fig. 3. Data are presented for $\beta=2$ (solid line, slope~average of the three $\text{Log}_2[DNA]$ values used to calculate the $C_{T\text{int ideal } k}=25.7$) or ten (dashed line, slope~average of three $\text{Log}_{10}[DNA]$ used to calculate the $C_{T\text{int ideal } k}=7.72$)

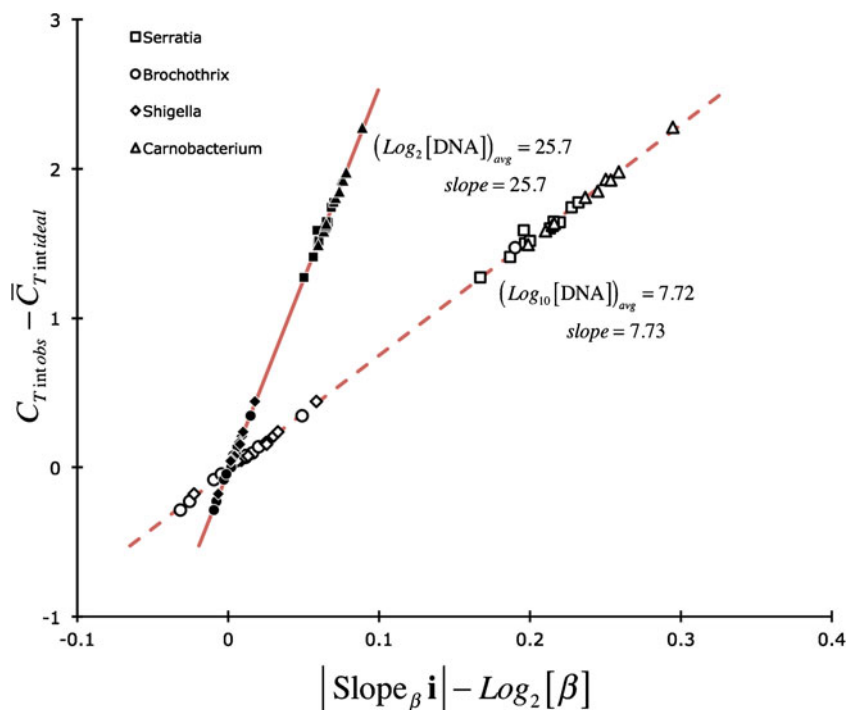


Fig. 5 Deviations from ideality for the C_{Ti} versus $\text{Log}_\beta[\text{DNA}]_i$ intercepts (Y -axis) and $|\text{slopes}|$ (X -axis) derived from the linear regression parameters associated with individual (k) experimental components of Fig. 4 (ten experimental repeats each of four isolate stnds). The slopes of these relationships exactly match the base β logarithm of the DNA concentration used to calculate the ideal C_T versus $\text{Log}_\beta[\text{DNA}]_{\text{fixd}}$ intercept where $[\text{DNA}]_{\text{fixd}} = 10^4, 10^5, 10^6, 10^7,$ and 10^8 copies per assay

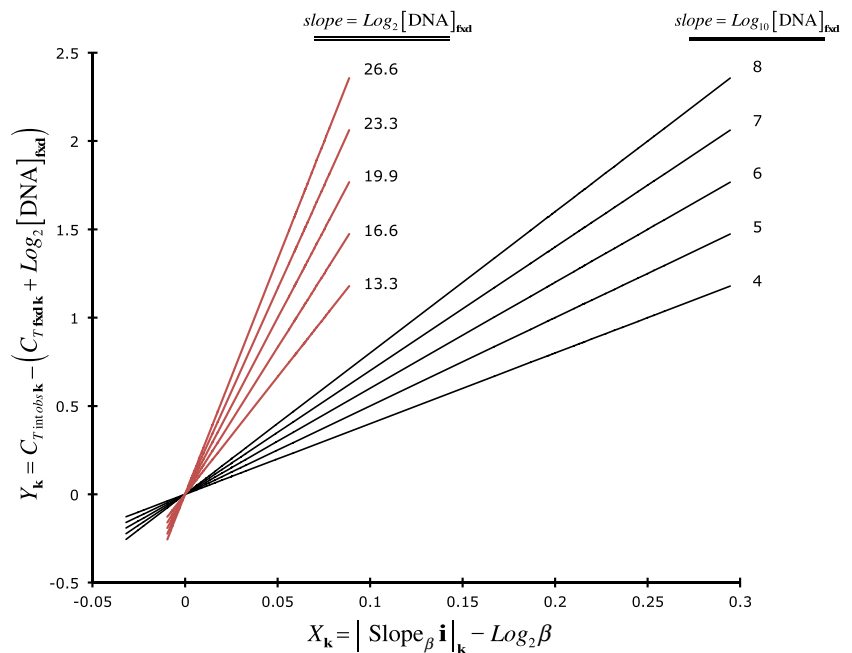


Fig. 5 can only result from the simplification of Eq. 7 since this defines the slope (or “regression coefficient”; all summations are taken from $k=1$ to $k=K$; e.g., in Fig. 5, $K=40$ experiments) of lines using standard linear regression [15]

$$\begin{aligned} \left(\frac{\partial Y}{\partial X}\right)_{\text{fixd}} &= \frac{\sum X_k Y_k - \frac{(\sum X_k)(\sum Y_k)}{K}}{\sum X_k^2 - \frac{(\sum X_k)^2}{K}} \\ &= \text{Log}_\beta[\text{DNA}]_{\text{fixd}} \end{aligned} \tag{7}$$

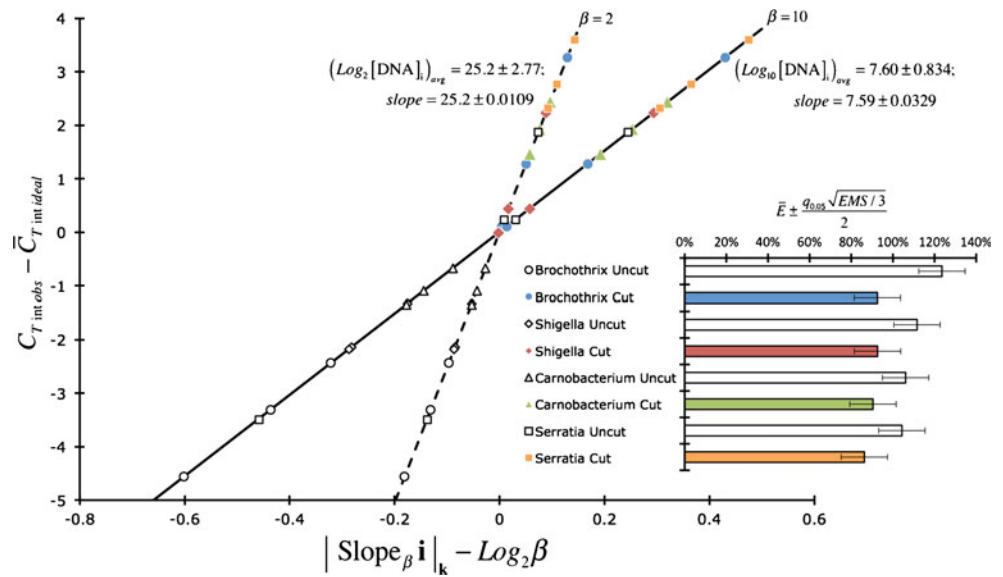
where $X_k = \{|\text{Slope}_\beta i_k| - \text{Log}_2 \beta\}$ and $Y_k = \{C_{T \text{ int obs } k} - C_{T \text{ int ideal } k}\} = \{C_{T \text{ int obs } k} - (C_{T \text{ fixd}} + \text{Log}_2[\text{DNA}]_{\text{fixd}})\}$.

Symbolically, the simplification of Eq. 7 is not possible and the relationships can only be discerned from the numerical outcome (e.g., via the “LINEST” function in MS Excel), as shown in Fig. 5. It is evident that any particular standard DNA concentration can only enter into Eq. 7 because it is involved in defining $C_{T \text{ int ideal}}$. Lastly, it is important to emphasize that while $\partial Y/\partial X$ is always β -modulated, $C_{T \text{ int ideal}}$ is base 2-regulated (Eq. 6).

A similar formulaic result to that seen in Figs. 4 and 5 was observed (Fig. 6) when these four 16S rDNA PCR products were “cloned,” extracted, \pm restriction enzyme-digested, purified, and the qPCR experiments rerun (three experimental replicates per treatment combination; three $\phi = 0.1$ serial dilutions per observation set, whereupon the average $[\text{DNA}]_{i=0}$ was $\sim 4 \times 10^8$ copies per assay). The terms “cut” and “uncut” refer to *Bam*HI restriction enzyme digestion (see “Materials and methods”) of the plasmids which contain the cloned rRNA genes and a *Bam*HI restriction site

residing outside the cloned gene. We found larger than expected perturbations in $\{C_{T \text{ int obs}} - C_{T \text{ int ideal}}\}$ and $|\text{Slope}_\beta i| - \text{Log}_2 \beta$, thereby allowing a more rigorous test of our hypothesis: that is, the slope of $\{C_{T \text{ int obs}} - C_{T \text{ int ideal}}\}$ as a function of $|\text{Slope}_\beta i| - \text{Log}_2 \beta$ is *always* the base β logarithm of the $[\text{DNA}]$ values used to calculate $C_{T \text{ int ideal}}$ (Eq. 6). As seen previously (Figs. 4 and 5), the observed slopes in Fig. 6 (25.2 ± 0.0109 and 7.59 ± 0.0329 for $\beta=2$ and 10, respectively) were equivalent to the average $\text{Log}_\beta[\text{DNA}]_i$ (25.2 and 7.60 for $\beta=2$ and 10, respectively), whereupon $[\text{DNA}]_i$ represents the three stnd concentrations ($i=0, 1, 2$) used in calculating $C_{T \text{ int ideal}}$ (Eq. 6). Generally, these qPCR parameter deviations from ideality shown in Fig. 6 were greater (i.e., the total $Y = \{C_{T \text{ int obs}} - C_{T \text{ int ideal}}\}$ range ~ 8) than those shown in Fig. 4 (the total $Y = \{C_{T \text{ int obs}} - C_{T \text{ int ideal}}\}$ range ~ 3). A significant part of this observation is due to the fact that the between-replicate variation was greater. For instance, the inset within Fig. 6 shows the variability in \bar{E} for all the cloned isolates and demonstrates the relatively large variation between replicated experiments (unlike previous results, inset in Fig. 3). Also, the “cut” plasmids had $\{C_{T \text{ int obs}} - C_{T \text{ int ideal}}\}$ values which were mainly positive (i.e., $\text{obs} > \text{ideal}$; 11 of 12 observations positive) and were similar to the rRNA amplified gene products (i.e., linear DNA) previously used. Contrariwise, for the 16S rRNA gene on the “uncut” plasmids, the $\{C_{T \text{ int obs}} - C_{T \text{ int ideal}}\}$ values were mostly negative (i.e., $\text{obs} < \text{ideal}$; 10 of 12 observations negative). Clearly, regardless of the mechanism, there can be (Fig. 6) substantial deviations in the target DNA concentration dependence associated with samples with a different preparatory provenance. Rather than attempting to minimize these differences, one can, knowing only $|\text{Slope}_\beta j|$,

Fig. 6 Deviations from ideality for the C_{Ti} versus $\text{Log}_\beta[\text{DNA}]_i$ intercepts (Y -axis) and $|\text{slopes}|$ (X -axis). The DNA used for these experiments were from various dilutions of cloned 16S rDNA amplicons+restriction enzyme cutting. The inset bar graph adjacent to the figure legend represents the various PCR efficiencies (Eq. 5) showing that (except for *Brochothrix*) all are statistically similar (those means with overlapping error bars are *not* significant at the $P=0.05$ level), albeit uncut are nearly always greater than uncut E values



calculate an associated $C_{T \text{ int predicted}}$ (Eq. 8a) with some accuracy knowing only $C_{T \text{ int ideal}}$ (Eq. 6) obtained from one, or more, PCR std solutions.

$$C_{T \text{ int predicted}} = \text{Log}_\beta[\text{DNA}]_i \times (|\text{Slope}_\beta j| - \text{Log}_2 \beta) + C_{T \text{ int ideal}} \tag{8a}$$

Estimation of $[\text{DNA}]_{\text{unk}}$

All of our results (Figs. 4, 5, and 6) argue that a predicted C_{Ti} versus $\text{Log}_\beta[\text{DNA}]_i$ intercept (Eq. 8a) can be used with the unk solution’s $\text{Slope}_\beta j$ as a corrected std curve. To test this further, we created a hypothetical array of C_{Ti} versus $\text{Log}_\beta[\text{DNA}]_i$ data with a poor efficiency ($E=78.7\%$; Fig. 7) and compared the formulaically generated (i.e., $C_{T \text{ int ideal}}$ and $C_{T \text{ int predicted}}$ derived from each $[\text{DNA}]_i$) with the observed (from linear regression) intercept. The thin blue lines associated with each data point in Fig. 7 are those displaying an ideal slope ($-\text{Log}_2 \beta$; Eq. 3) and intercept ($C_{Ti} + \text{Log}_2[\text{DNA}]_i$; Eq. 6) with an origin at $\{X, Y\} = \{\text{Log}_\beta[\text{DNA}]_i, C_{Ti}\}$. The heavy, dashed line is the semi-log regression expression for these $[\text{DNA}]_i$ data points and associated C_{Ti} . The insert figure shows a blowup of the plot and, on the Y -axis, the 6 $C_{T \text{ int predicted}}$ (Eq. 8a, red circles) at $[\text{DNA}]_i = 1$ copy per assay (i.e., $\text{Log}_\beta[1] = 0$) and shows that *any* of these *predicted intercepts* is approximately equivalent to the intercept associated with linear regression (i.e., $C_{T \text{ int obs}}$ when $r^2 \sim 1$).

For qPCR estimation of an unk DNA concentration (i.e., $[\text{DNA}]_{\text{unk}} = [\text{DNA}]_{j=0}$), we suggest the following protocol illustrated in Fig. 8. Use three, or more, unk dilutions (0.1^j , with $j=0, 1,$ and 2) and collect the associated three C_{Tj} in

order to calculate $\text{Slope}_\beta j$ and E_{unk} (Eq. 5). Use enough std solution dilutions of each purified amplicon of choice to bracket the observed C_{Tj} range (Fig. 8, multiplication symbols). Calculate the $\text{Slope}_\beta i$ and associated intercept ($C_{T \text{ int obs}}$) as well as E_{std} . Calculate a $C_{T \text{ int ideal}}$ (Eq. 6), whereupon the $[\text{DNA}]_i$ value in Eq. 6 is extrapolated from the standard curve using the unk’s C_{Tj} (i.e., $C_{T \text{ int ideal}} = C_{Tj} + \text{Log}_2[(1 + E_{\text{std}})^{C_{T \text{ int obs}} - C_{Tj}}]$; Fig. 8, gray circles). Knowing both $C_{T \text{ int ideal}}$ and the slope of the C_{Tj} versus $\text{Log}_\beta \phi^j$ plot (i.e., $\text{Slope}_\beta j$), one can calculate each j th $C_{T \text{ int predicted}}$ using a modified version of Eq. 8a

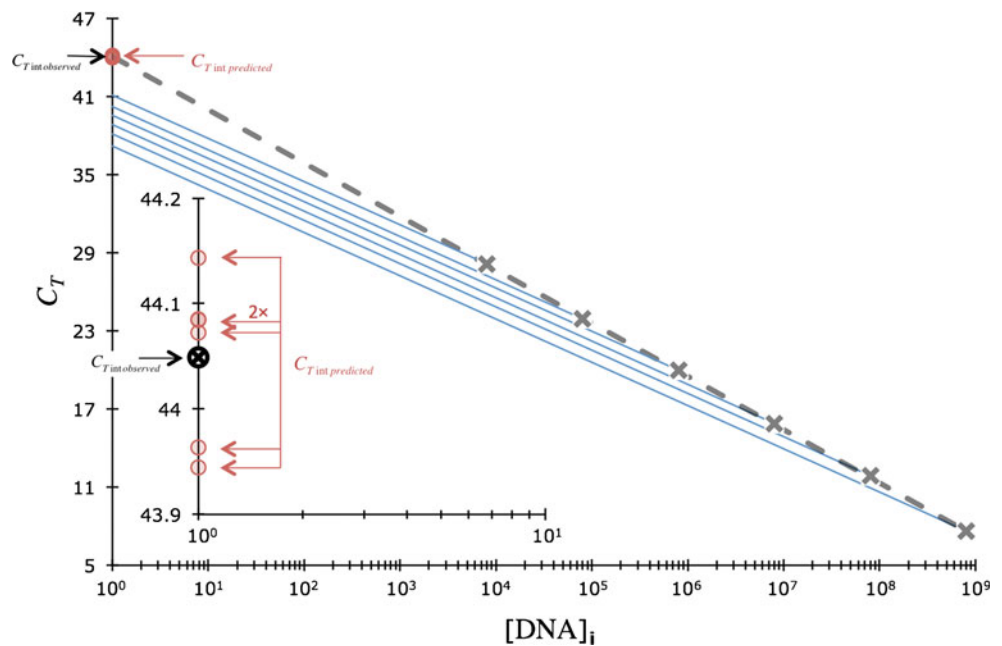
$$C_{T \text{ int predicted } j} = \text{Log}_\beta \left[(1 + E_{\text{std}})^{C_{T \text{ int obs}} - C_{Tj}} \right] \times (|\text{Slope}_\beta j| - \text{Log}_2 \beta) + \left(C_{Tj} + \text{Log}_2 \left[(1 + E_{\text{std}})^{C_{T \text{ int obs}} - C_{Tj}} \right] \right). \tag{8b}$$

It should be noted that $(1 + E_{\text{std}})^{C_{T \text{ int obs}} - C_{Tj}}$ in Eq. 8b ($= \beta^{(C_{T \text{ int obs}} - C_{Tj}) \div \text{Slope}_\beta i}$) is the traditional method (method A) for calculating $[\text{DNA}]_{\text{unk}}$ at any particular unk dilution j . Equation 8b simplifies to

$$C_{T \text{ int predicted } j} = C_{Tj} - \left(\text{Slope}_\beta j \times \text{Log}_\beta \left[(1 + E_{\text{std}})^{C_{T \text{ int obs}} - C_{Tj}} \right] \right). \tag{8c}$$

The $\bar{C}_{T \text{ int predicted}}$ is then calculated from the average of the three or more unk j ($j=0, 1, \dots, J$) $= C_{T \text{ int predicted}}$ values.

Fig. 7 Hypothetical array of C_{Ti} versus $\text{Log}_\beta[\text{DNA}]_i$ data calculated to have a poor efficiency ($E=78.7\%$) used for comparing the formulaically generated [i.e., $C_{T \text{ int ideal}}$ (Eq. 3) and $C_{T \text{ int predicted}}$ (Eq. 6) derived from each $[\text{DNA}]_i$] with the observed ($C_{T \text{ int obs}}$ from linear regression) intercepts. The inset is a blowup of the Y-axis showing the six $C_{T \text{ int predicted}}$ values (Eq. 8a) in red relative to the $C_{T \text{ int obs}}$ (in black, circle with cross) calculated from linear regression of C_{Ti} as a function of $\text{Log}_\beta[\text{DNA}]_i$



The unk DNA solutions (or $[\text{DNA}]_j$) can then be estimated (method B) from C_{Tj} and $\text{Slope}_{\beta j}$ as (Fig. 8, circles)

$$[\text{DNA}]_{jB} = \beta^{\frac{C_{Tj} - \bar{C}_{T \text{ int predicted}}}{\text{Slope}_{\beta j}}} = (1 + E_{\text{unk}})^{\bar{C}_{T \text{ int predicted}} - C_{Tj}} \quad (9)$$

An example set of observations is provided in Fig. 8 for a relatively dilute set of *Brochothrix* 16S rDNA ($E_{\text{std}}=0.922 \pm 0.0153$, $E_{\text{unk}}=1.05 \pm 0.0592$) and shows that the degree of difference between the traditional and the above estimation of $[\text{DNA}]_{\text{unk}j}$ using Eqs. 8c and 9 is approximately $\pm 40\%$.

To illustrate some of the potential ramifications of this technique, Table 1 provides data generated with a variable

E_{std} and fixed E_{unk} . Thus, the hypothetical C_{Ti} s with $\text{Log}_\beta[\text{DNA}]_i$ and C_{Tj} s with $\text{Log}_\beta[\text{DNA}]_j$ data pairs were calculated to have varying degrees of difference between their E values: $\delta C_{Ti} = C_{Ti} - C_{Ti-1} = \text{Log}_{(1+E_{\text{std}})} \beta$ for E_{std} s between 0.7 and 1.1 in increments of 0.1 and $\delta C_{Tj} = 3.92$ ($E_{\text{unk}} \sim 0.8$). We have extended these calculations over a highly unlikely range in $E_{\text{std}} - E_{\text{unk}}$ (ΔE) to view the extent of relative change in $[\text{DNA}]_{\text{unk}}$ as a function of ΔE . The obvious point to belabor is that the closer E_{unk} is to E_{std} , the closer the ratio of the calculated $[\text{DNA}]_{\text{unk}A} \div [\text{DNA}]_{\text{unk}B}$ are to unity. Also, for this model, $[\text{DNA}]_{j=0A} \div [\text{DNA}]_{j=0B}$ increases as a quadratic ($f_{A/B} = 1.762 \Delta E^2 +$

Fig. 8 Plot of *Brochothrix* 16S rDNA std (multiplication symbol, dotted line) and unk (method A—gray circle, dotted line; method B—black circle, solid line) threshold cycle numbers (C_T) as a function of $[\text{DNA}]$

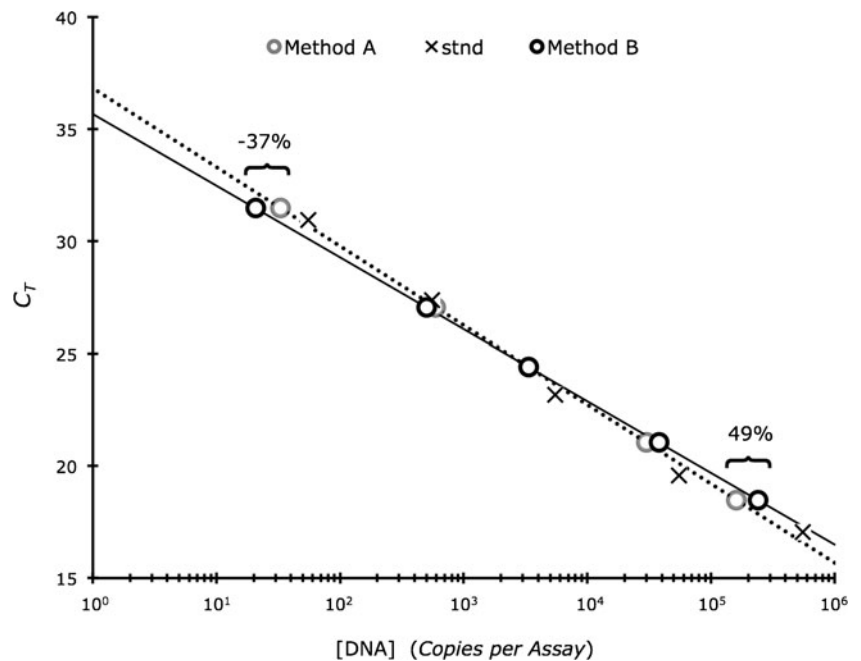


Table 1 Relationship between the traditional (method A: $(1 + E_{std})^{C_{T_{int}^{obs}} - C_{T_j=0}}$) and subject (method B: Eqs. 8a, 8b, 8c, and 9) technique for estimating $[DNA]_{unkj=0}$

$E_{std} - E_{unk}$	$[DNA]_{unkj=0}$			A/B	$\partial_{\Delta E} f_{A/B}$
	Method A	Method B	B from $f_{A/B}$ ^a		
0.3	1.88×10^6	1.03×10^6	1.03×10^6	1.83	3.63
0.2	2.77×10^6	1.83×10^6	1.83×10^6	1.51	3.28
0.1	4.15×10^6	3.36×10^6	3.35×10^6	1.24	2.92
0	6.36×10^6	6.36×10^6	6.36×10^6	1	2.57
-0.1	9.99×10^6	1.25×10^7	1.26×10^7	0.799	2.22
-0.2	1.61×10^7	2.56×10^7	2.57×10^7	0.630	1.87
-0.3	2.69×10^7	5.49×10^7	5.45×10^7	0.490	1.51

The predicted $[DNA]_{j=0}$ B was calculated from the rearrangement of the fitting function ($f_{A/B}$). The most likely scenario would be within the $E_{std} - E_{unk}$ range = 0.1–0.3

$E_{unk} = 0.8$; $C_{T_j=0} = 13.9$

^a fitting function = $f_{A/B} = [DNA]_{j=0A} \div [DNA]_{j=0B} = 1.762\Delta E + 2.219\Delta E + 1$

$$[DNA]_{j=0B} = \frac{1,000[DNA]_{j=0A}}{1,000 + \Delta E(2.219 + 1.762\Delta E)}$$

$2.219\Delta E + 1$, $r^2 \sim 1$) function of ΔE in such a way that each incremental increase in ΔE shows an ever-growing increase in the ratio of the two $[DNA]_{unk}$ calculation ($\partial_{\Delta E} f_{A/B}$ increases with ΔE ; Table 1) variants discussed herein. These data indicate that when $|\Delta E| > 0.1$, the relative change in the calculated DNA concentration with respect to method A is ± 20 –60%.

The data in Table 2 represent averages ($n = 10$) of replicated qPCR experiments each performed with five to seven dilutions of both std (different solutions than those utilized in Figs. 3, 4, and 5, but prepared identically) and unk (crude PrepMan Ultra DNA extracts of the same isolates) solutions so that direct statistical comparisons could be made. Table 2 presents an instance where two of the organism’s (*Brochothrix* and *Shigella*) E_{unk} s were found to be significantly different from their corresponding E_{std} . From these data, the traditional

Table 2 Absolute value of Slope $_{\beta i}$ ($|\partial C_T / \partial \text{Log}_{\beta} \phi^i|$) and Slope $_{\beta j}$ ($|\partial C_T / \partial \text{Log}_{\beta} \phi^j|$) and associated efficiencies (all 16S rDNA amplicons) as a function of source genome

Organism	Slope $_{\beta i}$	Slope $_{\beta j}$	E_{std}	E_{unk}	P
<i>Brochothrix</i>	3.44	3.07	0.953	1.12	1.39×10^{-6}
<i>Shigella</i>	3.44	2.84	0.952	1.25	8.66×10^{-6}
<i>Carnobacterium</i>	3.60	3.67	0.895	0.873	0.227
<i>Serratia</i>	3.72	3.42	0.857	0.959	6.08×10^{-5}

Each organism’s cell-free extract and associated standards were replicated ten times using a different one-way analysis of variance [20] for each organism, whereupon P is the probability that the averages in each row are equivalent. These amplicons are not from the same lot as those associated with Figs. 4, 5, and 6

procedure for determining the unknown DNA concentration (method A: $[DNA]_{unkA} = (1 + E_{std})^{C_{T_{int}^{obs}} - C_{T_j=0}}$) overestimates $[DNA]_{unk}$ relative to method B (Eqs. 8a, 8b, 8c, and 9; Table 3) when E_{unk} is significantly greater than E_{std} (Table 2). Four analyses of variance (completely randomized design, i.e., one-way classification with equal replication) [20] comparing the traditional (method A) with our process (method B) for estimating $[DNA]_{unk}$ from std solutions (from data in Table 2) for the four organisms are displayed in Table 3. In this specific case, the two significantly different unknown $[DNA]$ s were overestimated on average nearly two-fold from the standard method, and the larger the difference between Slope $_{\beta i}$ (std) and Slope $_{\beta j}$ (unk), the greater this misestimation was. For *Carnobacterium* ($E_{std} \sim E_{unk}$), either method was equivalent ($[DNA]_{unkA} \sim 1.72 \times 10^6$, $[DNA]_{unkB} \sim 1.64 \times 10^6$).

Conclusion

In this work, we have shown that the deviation of the C_{T_i} versus $\text{Log}_{\beta}[DNA]_i$ slopes and intercepts from ideality produces a linear relationship with a slope equal to the base β Logarithm of the std concentration utilized to calculate $C_{T_{int}^{ideal}}$ (Eq. 6). This point was illustrated when the predicted $C_{T_{int}}$ (Eq. 8a) was calculated for several different std $[DNA]_i$ with a poor qPCR efficiency and found that the average $C_{T_{int}^{predicted}}$ was equivalent to the intercept calculated from the linear regression estimate ($C_{T_{int}^{obs}}$). Because of this dependency, one is able to calculate a predicted $C_{T_{int}}$ based upon std qPCR responses which can be used with the unk’s Slope $_{\beta j}$ to “tweak” the traditional protocol (method A) to take into account differences in Slope $_{\beta i}$ and Slope $_{\beta j}$ (Fig. 8). Lastly, we show (Tables 2 and 3) that when Eqs. 8c and 9 are applied to actual unk DNA extracts from various organisms, the differences between methods A and B are statistically significant only when $\Delta E > 0.1$.

Table 3 Utilization of data from Table 2 in estimating $[DNA]_{unkj=0}$ using the traditional (method A: $[DNA]_{unkj=0} = (1 + E_{std})^{C_{T_{int}^{obs}} - C_{T_j=0}}$) and the proposed (method B: Eqs. 8a, 8b, 8c, and 9) techniques for back-calculating unknown DNA concentration from C_{T_j} (unk) observations

Organism	$[DNA]_{unk}$ (copies per assay)		P
	Method A	Method B	
<i>Brochothrix</i>	2.62×10^6	3.84×10^6	3.49×10^{-3}
<i>Shigella</i>	1.74×10^7	3.39×10^7	1.33×10^{-3}
<i>Carnobacterium</i>	1.72×10^6	1.64×10^6	0.806
<i>Serratia</i>	2.02×10^7	2.56×10^7	0.173

P is the probability that log-transformed $[DNA]_{unkj=0}$ within each row are equivalent

References

1. Chien A, Edgar DB, Trela JM (1976) Deoxyribonucleic acid polymerase from the extreme thermophile *Thermus aquaticus*. *J Bacteriol* 127:1550–1557
2. Bartlett JMS, Stirling D (2003) A short history of the polymerase chain reaction. *Methods Mol Biol* 226:3–6
3. Rabinow P (1996) Making PCR: a story of biotechnology. University of Chicago Press, Chicago, pp 6–7
4. Mackay IM (2004) Real-time PCR in the microbiology laboratory. *Clin Microbiol Infect* 10:190–212
5. Livak KJ, Schmittgen TD (2001) Analysis of relative gene expression data using real-time quantitative PCR and the $2^{-\Delta\Delta C_t}$ method. *Methods* 25:402–408
6. Yuan JS, Reed A, Chen F, Stewart CN Jr (2006) Statistical analyses of real-time PCR data. *BMC Bioinform* 7:85–96
7. He Y, Yao X, Gunther NW, Xie Y, Tu S-I, Shi X (2010) Simultaneous detection and differentiation of *Campylobacter jejuni*, *C. coli*, and *C. lari* in chickens using a multiplex real-time PCR assay. *Food Analytical Methods* 3:321–329
8. Bustin SA (2000) Absolute quantification of mRNA using real-time reverse transcription polymerase chain reaction assays. *J Mol Endocrinol* 25:169–193
9. Irwin PL, Nguyen L-HT, Chen C-Y (2010) The relationship between purely stochastic sampling error and the number of technical replicates used to estimate concentration at an extreme dilution. *Anal Bioanal Chem* 398:895–903
10. Pfaffli NW (2001) A new mathematical model for relative quantitation in real-time RT-PCR. *Nucleic Acids Res* 29:2002–2009
11. Schnell S, Mendoza C (1997) Theoretical description of the polymerase chain reaction. *J Theor Biol* 188:313–318
12. Ruijter JM, Ramakers C, Hoogaars WMH, Karlen Y, Bakker O, van den Hoff MJB, Moorman AFM (2009) Amplification efficiency: linking baseline and bias in the analysis of quantitative PCR. *Nucleic Acids Res* 37:1–12
13. Raeymaekers L (2000) Basic principles of quantitative PCR. *Mol Biotechnol* 15:115–122
14. Schnell S, Mendoza C (1997) Enzymological considerations for a theoretical description of the quantitative competitive polymerase chain reaction. *J Theor Biol* 184:433–440
15. Zar JH (1999) Biostatistical analysis. Prentice Hall, Upper Saddle River, pp 328–330
16. Irwin PL, Nguyen L-HT, Chen C-Y, Paoli G (2008) Binding of nontarget microorganisms from food washes to anti-*Salmonella* and anti-*E. coli* O157 immunomagnetic beads: most probable composition of background Eubacteria. *Anal Bioanal Chem* 391:525–536
17. Cottrell MT, Kirchman DL (2000) Community composition of marine bacterioplankton determined by 16S rRNA gene clone libraries and fluorescence in situ hybridization. *Appl Environ Microbiol* 66:5116–5122
18. Ririe KM, Rasmussen RP, Wittwer CT (1997) Product differentiation by analysis of DNA melting curves during the polymerase chain reaction. *Anal Biochem* 245:154–160
19. Morrison TB, Weis JJ, Wittwer CT (1998) Quantification of low-copy transcripts by continuous SYBR Green I monitoring during amplification. *Biotechniques* 24:954–962
20. Steele RGD, Torrie JH (1960) Principles and procedures of statistics. McGraw-Hill, New York, 481 pp